

# Shot-gather Reconstruction using a Deep Data Prior-based Neural Network Approach

## Reconstrucción de fuentes sísmicas usando un enfoque de Redes Neuronales Profundas de Datos Previos

Luis Rodríguez-López <sup>1a</sup>, Kareth León-López <sup>1b</sup>, Paul Goyes-Peñañiel <sup>1c</sup>, Laura Galvis <sup>1d</sup>, Henry Arguello <sup>1e</sup>

<sup>1</sup> Department of Systems Engineering and Informatics, Universidad Industrial de Santander, Colombia. Orcid: 0009-0003-4677-2161 <sup>a</sup>, 0000-0002-0502-9107 <sup>b</sup>, 0000-0003-3224-3747 <sup>c</sup>, 0000-0002-9232-7865 <sup>d</sup>, 0000-0002-2202-253X <sup>e</sup>. Emails: [luis2172004@correo.uis.edu.co](mailto:luis2172004@correo.uis.edu.co) <sup>a</sup>, [kareth.leon@correo.uis.edu.co](mailto:kareth.leon@correo.uis.edu.co) <sup>b</sup>, [ypgoype@correo.uis.edu.co](mailto:ypgoype@correo.uis.edu.co) <sup>c</sup>, [lavigal@correo.uis.edu.co](mailto:lavigal@correo.uis.edu.co) <sup>d</sup>, [henarfu@uis.edu.co](mailto:henarfu@uis.edu.co) <sup>e</sup>

Received: 17 April 2023. Accepted: 27 June 2023. Final version: 30 August 2023.

### Abstract

Seismic surveys are often affected by environmental obstacles or restrictions that prevent regular sampling in seismic acquisition. To address missing data, various methods, including deep learning techniques, have been developed to extract features from complex information, albeit with the limitation of requiring external seismic databases. While previous works have primarily focused on trace reconstruction, missing *shot-gathers* directly impact the seismic processing flow and represent a major challenge in seismic data regularization. In this paper, we propose DIPsgr, a seismic *shot-gather* reconstruction method that uses only the incomplete seismic acquisition measurements to estimate their missing information employing unsupervised deep learning. Numerical experiments on three databases demonstrate that DIPsgr recovers the complete set of traces in each *shot-gather*, with preserved information and seismic events.

**Keywords:** Seismic data regularization; deep learning; unsupervised learning; shot-gather reconstruction; deep image prior; seismic processing; subsampled survey; convolutional network; seismic acquisition; data interpolation.

### Resumen

Los levantamientos sísmicos usualmente se ven afectados por obstáculos o restricciones ambientales que impiden el muestreo regular en la adquisición sísmica. Por lo tanto, se han desarrollado diversos métodos para reconstruir estos datos faltantes, incluidos los métodos de aprendizaje profundo, los cuales permiten extraer características de información compleja, con la limitante de bases de datos sísmicos externos. Aunque otros trabajos se han enfocado principalmente en la reconstrucción de trazas, los disparos que no se pueden adquirir impactan directamente el flujo del procesamiento sísmico y representa un reto mayor en la regularización de datos sísmicos. En este trabajo proponemos DIPsgr, un método de reconstrucción de disparos sísmicos que usa solamente las medidas de las adquisiciones sísmicas incompletas para estimar la información faltante usando aprendizaje profundo no supervisado. Los experimentos numéricos con tres bases de datos muestran que DIPsgr recupera el conjunto completo de trazas en cada *shot-gather*, donde la información y los eventos sísmicos se conservan correctamente.

ISSN Printed: 1657 - 4583, ISSN Online: 2145 - 8456.

This work is licensed under a Creative Commons Attribution-NoDerivatives 4.0 License. [CC BY-ND 4.0](https://creativecommons.org/licenses/by-nd/4.0/)



How to cite: L. Rodríguez-López, K. León-López, P. Goyes-Peñañiel, L. Galvis, H. Arguello, "Shot-gather Reconstruction using a Deep Data Prior-based Neural Network Approach," *Rev. UIS Ing.*, vol. 22, no. 3, pp. 177-188, 2023, doi: <https://doi.org/10.18273/revuin.v22n3-2023013>

**Palabras clave:** regularización de datos sísmicos; aprendizaje profundo; aprendizaje no supervisado; reconstrucción de disparos sísmicos; imagen previa profunda; procesamiento sísmico; adquisición sub-muestreada; red neuronal convolucional; adquisición sísmica; interpolación de datos.

## 1. Introduction

Seismic data is used for imaging and to study the geological characteristics of the Earth through the propagation of waves generated by sources and measuring the signal response of the wavefield using receivers (i.e., geophones or hydrophones) [1]. The data collected in a seismic survey plays an essential role in the oil and gas industry and provides information to discover exploratory prospects. [1], [2]. Specifically, the seismic survey consists of arranging a set of sources that generate waves that propagate through the subsurface and whose energy is reflected and/or transmitted according to the physical properties of the rock layers. Then, the reflected energy that reaches the surface is captured by a set of receivers or geophones [2]. The coordinates of the sources and receivers with regular and dense separation make up the designed geometry (i.e., pre-plot). However, during the acquisition, the geometry may present variations due to operational, economic, or environmental factors, affecting the quality of the seismic design [1], [2], [3]. Precisely, the modifications in the original design led to a loss of some points of the regular grid. The resulting design from this process is known as a post-plot. The missing seismic data can be a set of receivers or even a complete *shot-gather*. Therefore, seismic data regularization (such as interpolation or reconstruction) is still a required and necessary step in seismic processing [4].

The state-of-the-art approaches in seismic data regularization have mainly focused on receiver reconstruction [5], [6], [7], [8]. Several techniques have been developed, such as methodologies based on filters on the wavefield operator, using transformation domains (Fourier) and algorithms based on sparsity priors [5], [6], [9], [10], [11]. Currently, in deep learning (DL), a variety of methods have been applied for the reconstruction of seismic data using different architectures for the computational learning model [12], [13], [14], [15]. DL has shown to be a useful tool for extracting features from the data and performing better interpolation compared to conventional methods [16]. A disadvantage of these DL-based reconstruction methods is the huge volumes of data required in the training process. This drawback arises because access to huge seismic data volumes is still limited. Therefore, a recent research area has proposed the application of new techniques that address this problem using only the data acquired for model training.

Currently, in the state-of-the-art, a DL methodology without external training data called deep image prior (DIP) has been proposed [17], also called DL from observed data, which only requires the data under observation or acquired and a convolutional neural network to extract all the necessary features for the task to be performed, such as reconstruction, denoising, or super-resolution. This helps to reduce the computational cost of training and, in turn, the large data sets required to generalize a model based on DL. DIP has been used in seismic applications for seismic data regularization, specifically, for the reconstruction of traces (i.e. receivers/geophones) with a convolutional neural network (CNN) [7], [8].

However, in more realistic applications, *shot-gathers* are also missing, and the current application of DIP is unable to extract features to recover a complete set of traces or *shot-gathers*, which is a more challenging task to solve. The problem could be adapted by taking the common-receiver gathers (receiver slice), where a *shot-gather* is represented by a trace, in which case, DIP does not consider the structures or characteristics of the seismic data along the receivers and shots dimensions.

This paper aims to reconstruct *shot-gathers* from incomplete measurements under the DL approach only from the observed data, focused directly on the current problems in seismic processing related to seismic data regularization. The proposed method DIPsgr was evaluated using field and synthetic seismic data acquired in *split-spread* and *inline offset* acquisition geometries.

## 2. DIPsgr: Deep Image prior-based Reconstruction Method

Let  $X \in \mathbb{R}^{M \times N \times L}$  denote the data collection from a dense and regular seismic acquisition with  $M$  time samples,  $N$  receivers, and  $L$  number of *shot-gathers*. We can mathematically model the subsampled data from an irregular or incomplete seismic acquisition as follows

$$Y = \Omega(X), \quad (1)$$

where  $Y \in \mathbb{R}^{M \times N \times L - S}$  is the acquired data with  $S$  missing *shot-gathers*. The subsampling functional operator  $\Omega(\cdot)$  extracts the acquired *shot-gathers* using the positions from the designed geometry.

Then, the reconstruction task consists of estimating  $X$  from  $Y$ . In unsupervised learning, the reconstruction problem can be modeled using a deep neural network  $M_\theta$  with trainable parameters  $\theta$  constrained by the loss function

$$L(\theta) = E(\Omega(M_\theta(Z)) - Y), \quad (2)$$

where  $E(\cdot)$  is a fidelity term and  $Z \in \mathbb{R}^{M \times N \times L}$  is a random noise realization with uniform distribution. The choice of random noise as input relies on that the implicit structure of the network  $M_\theta$  is considered as a prior in the process before learning the set of parameters  $\theta$  [17], and, then, the learning procedure yields  $M_\theta: Z \rightarrow X$ . Hence, in this approach, deep prior refers to the capability of  $M_\theta$  to estimate signals using only the measurements, avoiding huge labeled training data from external data sources.

The trainable parameters  $\theta$  can be optimized by minimizing Equation (2). The optimization problem is formulated as

$$\theta^* = \underset{\theta}{\operatorname{argmin}} \{L(\theta)\}, \quad (3)$$

where  $\theta^*$  are the optimal parameters of the deep neural network.

Finally, using the optimal parameters, the full and dense seismic data can be estimated as

$$X^* = M_{\theta^*}(Z), \quad (4)$$

where the neural network  $M_{\theta^*}$  works as a parametric function.

To guarantee the convergence of the optimization problem in Equation (3), the mean square error (MSE) is used as the fidelity term in Equation (2) and is denoted as

$$MSE(Y; \hat{Y}) = \frac{1}{MN(L-S)} \sum_{k=0}^{L-S-1} \sum_{j=0}^{N-1} \sum_{l=0}^{M-1} (Y_{i,j,k} - \hat{Y}_{i,j,k})^2 \quad (5)$$

where  $\hat{Y} = \Omega(M_\theta(Z))$ , during the unsupervised training.

Additionally, we have incorporated a constraint on the seismic signal in the frequency-wavenumber (FK) domain into the cost function. The FK domain is commonly used in seismic processing for analyzing spatial and temporal frequency content [18], [19]. Then, the objective is to find the optimal weights  $\theta^*$  of a solution in which the spatial and frequency attributes of  $\Omega(M_\theta(Z))$  and  $Y$  are close. Thus, the proposed cost

function is guided in both the spatial temporal (TX) and FK domains as follows:

$$L(\theta) = MSE(Y; \hat{Y}) + \lambda \cdot MSE(FK(Y); FK(\hat{Y})), \quad (6)$$

where  $FK$  represents the two-dimensional (2D) fast Fourier transform for every single measured *shot-gather* and  $\lambda$  is a compensation constant controlling the loss function in both domains. Despite the cost function constraining the output only to fit the measured data  $Y$ , the missing *shot-gathers* are suitably reconstructed in the optimization process since they share the same inner structure captured by the network through  $\theta$  during the optimization.

## 2.1. Reconstruction Algorithm

Algorithm 1 summarizes the DIPsgr method and shows the solution of Equation (3), where the objective is that the output of  $\Omega(M_\theta(Z))$  is the most similar to the acquired data  $Y$ . The inputs of the algorithm are:

- $Y$ : Acquired seismic data (incomplete *shot-gathers*).
- $\Omega$ : Subsampling operator that extracts *shot-gathers* using the known acquisition geometry.
- Epochs: Number of iterations for training.

Regarding the inputs of the algorithm, we remark that DIPsgr is based only on the acquired data in unsupervised learning.

Then, Algorithm 1 starts by generating a random noise  $Z$  with uniform distribution, followed by the random initialization of  $\theta$ . In steps 4–9 the network is trained in an unsupervised fashion using the Adam optimizer. Once the optimal parameters of the network are found in step 10, using the Equation (4), it is possible to reconstruct the best estimation of the seismic data set  $X^*$  using as input the noise from step 1. The architecture of the employed network  $M_\theta$  is described in section 2.2.

## 2.2. Neural Network Architecture

Figure 1 shows the scheme of the proposed architecture for reconstructing the *shot-gathers*. It consists of a 3D U-Net network, specifically an autoencoder type network with skip connections. The green arrows represent each convolutional layer with  $3 \times 3 \times 3$  filters, followed by a batch normalization and a sigmoid activation function. The red arrows represent the down sampling process, consisting of a convolutional layer with  $(3 \times 3 \times 3)$  filters

and a  $(2 \times 2 \times 2)$  stride to perform dimension reduction. The magenta arrows represent the up-sampling function that increases the spatial size using a bilinear interpolation. The gray arrows represent the skip connections at each level of the architecture. Finally, the yellow arrow represents the output layer as a convolutional layer with a  $(1 \times 1 \times 1)$  filter, followed by batch normalization and a sigmoid activation function. Each blue box represents activated feature maps across the architecture, and the number above defines the number of filters applied in the previous convolutional layer. Finally, the proposed network uses an input size of  $M \times N \times L$  equal to  $128 \times 128 \times 16$ , with a total of 3,156,835 trainable parameters.

---

**Algorithm 1** DIPsgrfor *shot-gather* reconstruction

---

Input:  $Y$ : acquired seismic data;  $\Omega$ : subsampling operator; Epochs.

- 1: Generate  $Z$  using an uniform distribution.
  - 2: Initialize  $\theta$  randomly
  - 3: for  $i = 1$  to Epochs do
  - 4:   Generate  $M_\theta(Z)$
  - 5:   Extract acquired *shot-gathers*  $\Omega(M_\theta(Z))$
  - 6:   Compute loss  $L(\theta)$  using Equation (6)
  - 7:   Update  $\theta$  using Adam optimizer
  - 8: end for
  - 9: Get the optimal parameters  $\theta^*$
  - 10:  $X^* \leftarrow M_{\theta^*}(Z)$    ▷ Estimate seismic data
- 
- Output: Reconstructed data  $X^*$
- 

### 3. Simulations and Results

This section presents the results obtained from the simulations for the reconstruction of *shot-gathers* at three different scenarios. We compare the performance of DIPsgr against three state-of-the-art reconstruction methods. The first one is a method for receiver reconstruction on 2D and 3D seismic data based on Internal Learning (IL) [20] using a CNN with 16 convolutional blocks (adapted here by adding more blocks to solve our reconstruction problem). The second one is the deep-seismic prior-based reconstruction (DSPRecon) algorithm, which is based on DIP [8]. The DSPRecon method was originally designed for trace reconstruction, nonetheless, for a fair comparison with the DIPsgr method, we transpose the seismic cube to work in the common-receiver-gather domain and recover the *shot-gathers* for every single receiver line, i.e., recovering the seismic *shot-gathers* for every single receiver array. The third method is the consensus equilibrium (CE) approach [21] that incorporates several regularizers in the optimization problem for recovering missing *shot-gathers*. Given that the CE approach outperforms the sparsity-based methods (see [21]), this paper disregards that comparison.

**Figure 2.** Statistical summary of 10 realizations to analyze the input noise  $Z$  generated from uniform, normal, and bernoulli distributions. The circles are outliers.

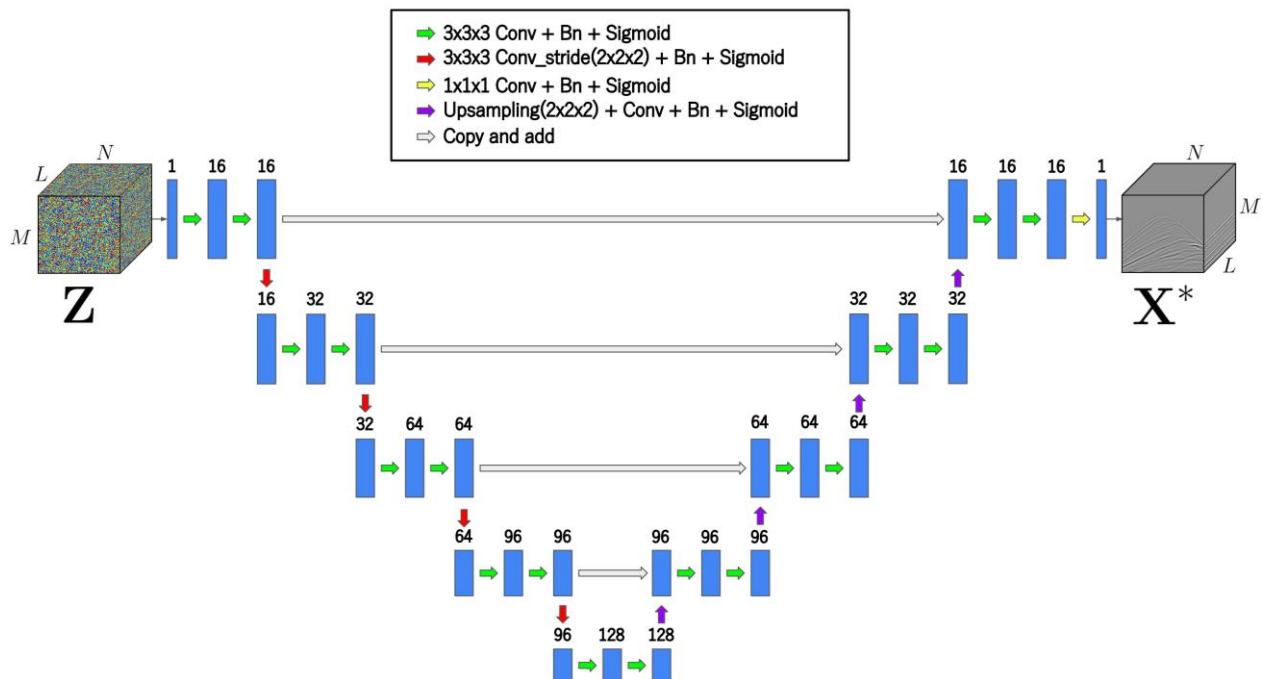


Figure 1. 3D U-Net architecture with random noise  $Z$  as the input for *shot-gather* reconstruction.

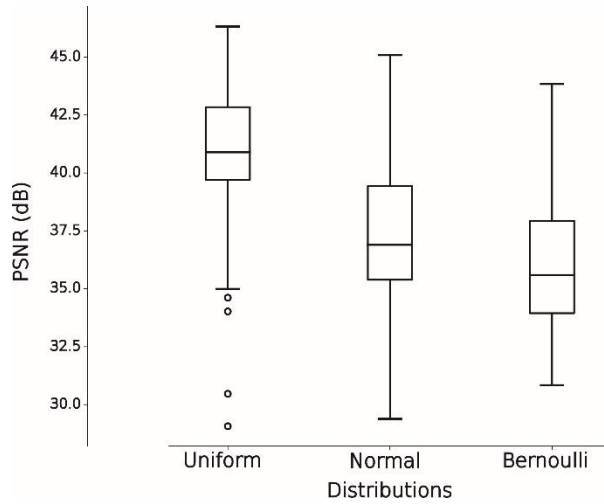


Figure 2. Statistical summary of 10 realizations to analyze the input noise  $Z$  generated from uniform, normal, and bernoulli distributions. The circles are outliers.

### 3.1. Seismic Datasets

We use three datasets, both field and synthetic, to test the DIPsgr method. We normalized all datasets between 0 and 1, as the output layer of the neural network employs the sigmoid activation function.

The synthetic datasets were simulated with DEVITO [22] using the acoustic Marmousi velocity model [23]. The acquisition geometry comprises 16 *shot-gathers* and 128 receivers; the energy source is a Ricker wavelet with a frequency of 10 Hz, and the trace length is 3000 ms. According to the position of the *shot-gathers* in the survey, we simulate the two following seismic acquisition geometries:

Dataset I: *Split-spread* acquisition with the shot in the middle of the receiver line. This dataset comprises  $L = 16$  *shot-gathers* with  $M = 128$  time samples and  $N = 128$  receivers.

Dataset II: *Inline offset* acquisition where the source is located at twice the receiver interval distance offset from the last hydrophone. This dataset comprises  $L = 16$  *shot-gathers* with  $M = 128$  time samples and  $N = 128$  receivers.

Dataset III: The field dataset is the well-known AVO Mobile Viking Graben [24], [25] survey from a marine acquisition. The original acquisition geometry comprises 249 *shot-gathers* and 120 receivers, the trace length is 6000 ms. The experiments were performed using the first 16 *shot-gathers* and resizing it to  $128 \times 128$  due to computational resources.

### 3.2. Metrics

To evaluate the quality of the reconstructed data with the DIPsgr method, we used the metrics Peak Signal-to-Noise Ratio (PSNR), and structural similarity index measure (SSIM) recommended by [21], [26]. PSNR is used to quantify the quality in terms of signal amplitude, and with SSIM, we account for the analysis of the structural features related to the shape of the waveforms i.e., hyperbolic and linear events recorded in the *shot-gathers*.

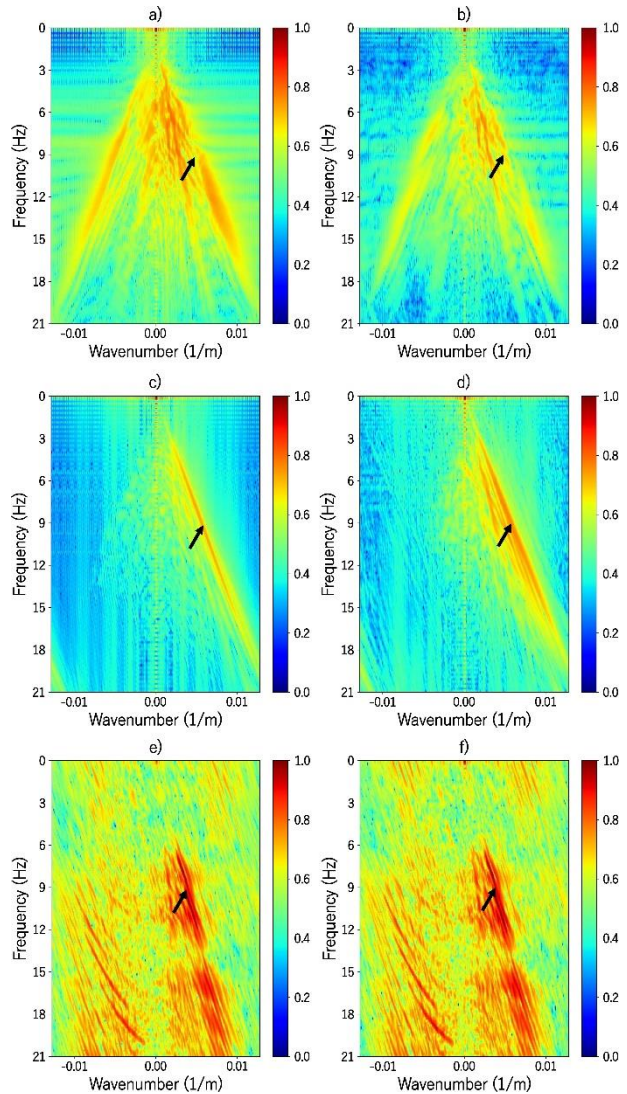


Figure 3. *Shot-gather* 8 in FK domain. Ground truth (a, c, e) and (b, d, f) interpolated with DIPsgr. The first, second, and third rows are datasets I, II, and III, respectively.

Table 1. Performance comparison of DIPsgr (proposed) and IL [20], DSPRecon [8], and CE [21] methods using the average PSNR and SSIM metrics

Experiment	Shot	PSNR (dB)				SSIM			
		DIPsgr	DSPRecon	IL	CE	DIPsgr	DSPRecon	IL	CE
Dataset I: Synthetic <i>split-spread</i>	4	38.93	26.27	16.20	15.06	0.990	0.760	0.420	0.661
	6	38.41	22.92	17.81	15.42	0.992	0.635	0.756	0.660
	8	37.77	20.55	17.37	12.97	0.991	0.509	0.541	0.618
	11	38.93	19.06	16.75	10.73	0.991	0.414	0.526	0.557
	13	37.68	20.43	15.92	12.36	0.990	0.473	0.369	0.607
	Average	38.34	21.85	16.81	13.31	0.991	0.558	0.522	0.620
Dataset II: Synthetic <i>inline offset</i>	4	42.78	21.23	15.56	17.28	0.995	0.623	0.616	0.841
	6	44.62	18.12	18.63	11.13	0.996	0.473	0.774	0.707
	8	44.87	17.27	16.19	15.21	0.997	0.353	0.574	0.815
	11	44.16	16.48	16.75	13.01	0.995	0.283	0.750	0.824
	13	43.41	17.08	17.13	15.66	0.995	0.308	0.663	0.841
	Average	43.97	18.03	16.85	14.46	0.996	0.408	0.676	0.806
Dataset III: AVO Mobil Viking Graben	4	35.19	25.78	14.65	22.34	0.973	0.730	0.277	0.552
	6	35.60	22.54	14.92	15.92	0.974	0.596	0.462	0.560
	8	36.69	21.09	14.43	21.88	0.979	0.499	0.307	0.562
	11	36.86	18.66	15.24	17.81	0.978	0.390	0.536	0.545
	13	33.98	20.12	14.62	22.89	0.971	0.443	0.365	0.580
	Average	35.37	21.64	14.77	20.17	0.974	0.532	0.389	0.560

### 3.3. Network Configuration

The training process was fixed with 3000 epochs for all experiments, using the Adam optimizer [27]. Additionally, for Dataset I and II, we included a learning rate starting at 0.01 with an exponential decay rate of 0.9 every 500 epochs. For the compensation constant  $\lambda$  of Equation (6), we found that the best choice is  $\lambda = 0.5$  by tuning the parameter over 10 Monte Carlo realizations with the field and synthetic datasets. Finally, for Dataset III, the learning rate was fixed at 0.001 and the compensation constant  $\lambda = 0.001$ . On the other hand, to choose the distribution for generating the random input noise that yields better reconstruction results, a set of experiments with 10 realizations was conducted consisting of the reconstruction of 5 *shot-gathers* using synthetic data and generating  $Z$  from uniform, normal, and bernoulli distributions. Figure 2 shows the statistical summary of the experiments in terms of PSNR from each distribution. The boxplots show that generating  $Z$  with a uniform distribution yields the best reconstruction scores with random values between 0 and 1.

### 3.4. Numerical Results

Table 1 summarizes the performance of the DIPsgr approach and the state-of-the-art methods, i.e., IL, DSPRecon, and CE, recovering *shot-gathers* from the three different datasets. The second column reports the corresponding index of the reconstructed *shot-gather*

from the given geometry. In general, note that the proposed method outperforms the other methods in terms of PSNR and SSIM and provides a better estimation for *shot-gather* reconstruction than the estimations achieved with comparison methods, where each of the comparative methods only requires the data acquired. Specifically, the proposed method is superior to the compared methods in up to 21.68 dB (PSNR) and 0.423 (SSIM) on average. The average best performance of our approach is in the Dataset II Synthetic *inline offset* with 43.97 dB (PSNR), which is related to the low complexity in the seismic features for a marine acquisition with abundant linear seismic events. On the other hand, in the same marine acquisition but in a field survey tested with Dataset III, the performance of our method is, on average, 35.37 dB (PSNR), keeping a good result, although the field data contains noise.

Moreover, we have conducted an assessment of the efficacy of our methodology using the reconstruction of *shot-gather* 8 in the frequency-wavenumber (FK) domain to showcase the capacity of our algorithm for the preservation of seismic characteristics in this domain, with regard to both the dips of the spectrum and the frequency range of the signal. Figure 3 illustrates the results of the reconstruction in the FK domain of the Datasets I, II, and III, where it can be observed that the reconstruction in this domain presents good quality. For Dataset I, we observed a spectral shift that resulted from

the algorithm's ability to reconstruct the *shot-gather* while applying filtering in the FK domain. This behavior is anticipated since DIPsgr method includes the FK domain as a regularization term, thereby facilitating network convergence by producing smoother and more continuous FK spectra. On the other hand, in Dataset III the signal complexity is preserved in the FK domain.

Figure 4 shows the reconstruction results obtained with the different methods using Dataset I. Note that reconstruction using the DIPsgr method (Figure 4b) presents a good performance in the preservation of seismic features, especially the feature located at 2–3 km and 2–3 s, pointed out with the arrow. Figure 5 shows the result with Dataset II, where the *shot-gather* 8 was reconstructed while adequately preserving the main linear event related to the direct water wave. Also, it can be noted that an internal linear event was highlighted and pointed with an arrow about 2–3 km away. The comparison methods reconstructions added artifacts causing structural changes in the gather; these can be seen in the normalized residual Figure 5(f–i). Figure 6 shows that DIPsgr adequately reconstructs the shotgather 8 from Dataset III, preserving the structural seismic waveforms. Particularly, those linear events between 1–2 km and 1–3 s, while the reflections are maintained.

#### 4. Discussion

Computational cost: DIPsgr method was more efficient in terms of quality and computational cost compared to other DL-based methods with 3'156'835', 1'424'643, and 368'523 trainable parameters. The computation time was 10 min, 164 min, and 80 s for DIPsgr, DSPRecon, and IL, respectively. It is worth noting that all computational experiments were conducted under the same conditions using a GPU Nvidia T4 Tensor Core.

Model Uncertainty: The experimental results presented in this study demonstrate the superior performance of the DIPsgr method for reconstructing *shot-gather* data from incomplete seismic acquisition compared to state-of-the-art methods. However, it is important to acknowledge that DIPsgr method is sensitive to the initialization of the network weights  $\theta$ . To investigate this sensitivity, a model uncertainty analysis was conducted by randomly initializing the weights and reconstructing five *shot-gathers* with fixed Z values across 100 realizations. Table 2 summarizes the reconstruction results on the field Dataset III using the DIPsgr method in terms of PSNR and SSIM, with a standard deviation of 1.98 dB in the PSNR. These results indicate that the reconstruction performance has a small deviation from the average, which may have implications for certain applications where consistent results are necessary (e.g., AVO, FWI, petrophysical parameter estimation).

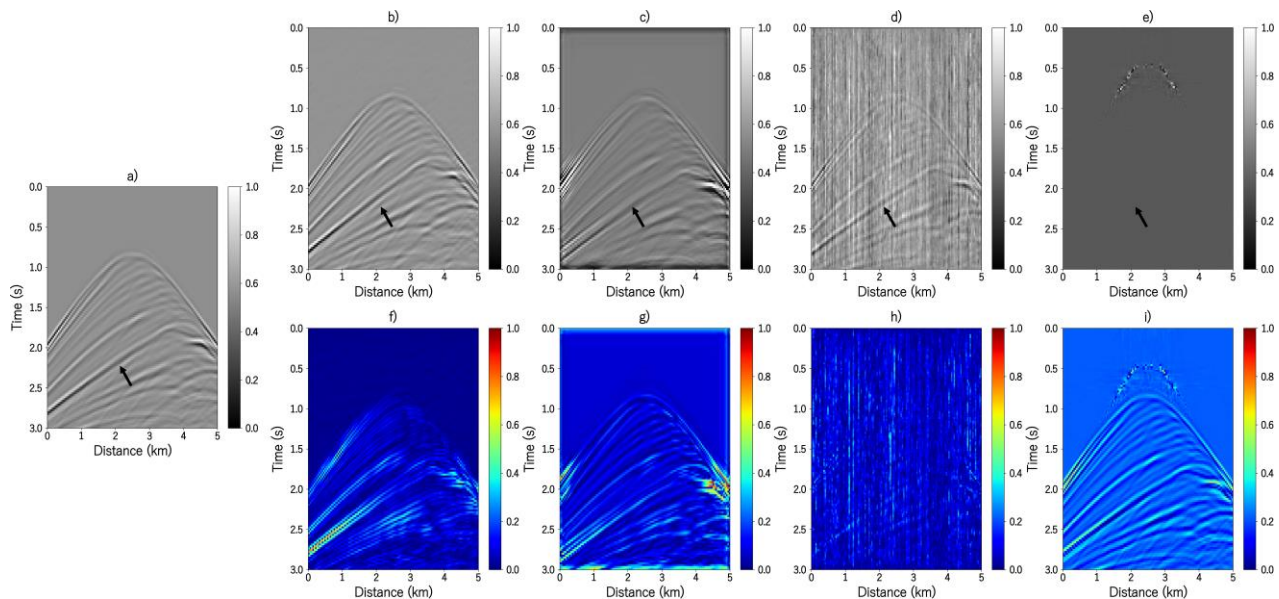


Figure 4. (a) Ground truth for the *shot-gather* 8 in Dataset I: Synthetic split-spread, and the interpolation results with (b) DIPsgr (proposed), (c) IL, (d) DSPRecon, and (e) CE method. (f–i) Normalized difference for each method, respectively.

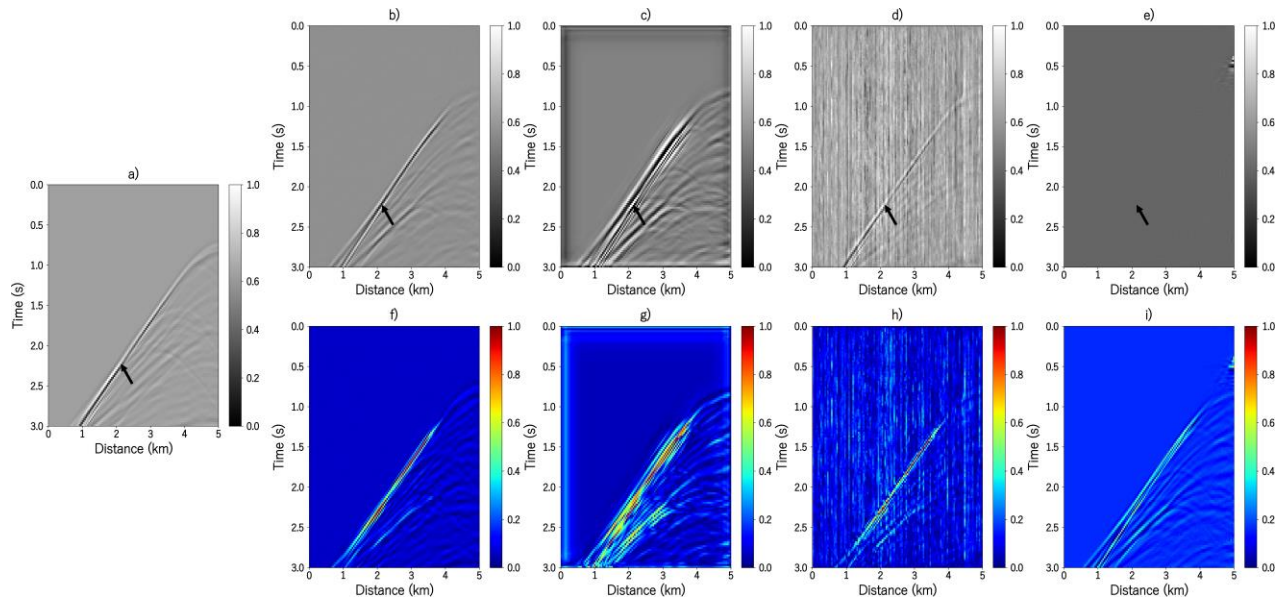


Figure 5. (a) Ground truth for the *shot-gather 8* in Dataset II: Synthetic inline offset, and the interpolation results with (b) DIPsgr, (c) IL, (d) DSPRecon, and (e) CE method. (f–i) Normalized difference for each method, respectively.

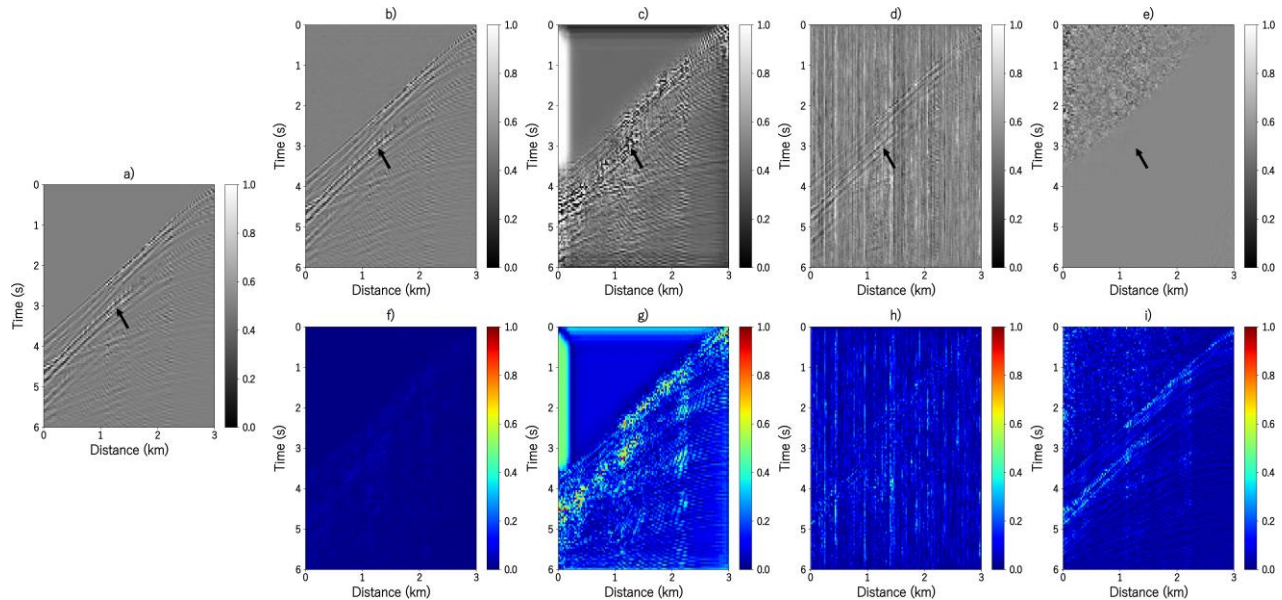


Figure 6. (a) Ground truth for the *shot-gather 8* in Dataset III: AVO Mobil Viking Graben, and the interpolation results with (b) DIPsgr, (c) IL, (d) DSPRecon, and (e) CE method. (f–i) Normalized difference for each method, respectively.

Moreover, the experiments presented in the Numerical Results section involve randomly initialized trainable parameters. Although our approach is inherently dependent on the observed data in a given area, fine-tuning is possible. For instance, one strategy is to train the network initially using a set of synthetic data and then

use these trained parameters as initialization for reconstructing field data. Since field data can be more complex, utilizing synthetic data initialization may lead to faster convergence compared to training from scratch. Therefore, further research is needed to develop robust

weight initialization methods to improve the overall performance and reliability of DIPsgr.

Table 2. Sensitivity analysis in the reconstruction neural network initialization of the DIPsgr method

	PSNR (dB)	SSIM
<b>Min</b>	28.13	0.887
<b>Average</b>	34.21	0.964
<b>Std.</b>	1.98	0.018
<b>Max</b>	38.18	0.985

## 5. Conclusions

This paper introduces a novel approach based on deep data priors for recovering missing *shot-gathers* in seismic data. By leveraging incomplete seismic acquisition and a 3D convolutional neural network, the DIPsgr method effectively captures important statistics and structural features from the data to reconstruct the missing *shot-gathers*. DIPsgr considers information in the temporal-spatial and frequency-wavenumber domains to preserve features in both domains, providing valuable insights for downstream data processing. Comparative experiments with state-of-the-art algorithms show that the DIPsgr method achieves outstanding results in both land and marine data. Notably, our approach differs from other deep image prior-based methods that mainly focus on trace reconstruction of 2D or 3D seismic data, as DIPsgr method is specifically designed to reconstruct a complete set of *shot-gathers*.

## Funding

This work was supported by project 110287780575 through the agreement 785-2019 between the Agencia Nacional de Hidrocarburos (ANH) and the Ministerio de Ciencia, Tecnología e Innovación (Minciencias) and Fondo Nacional de Financiamento para la Ciencia, la Tecnología y la Innovación Francisco José de Caldas.

## Autor Contributions

L. Rodríguez-López: Formal analysis, Writing Original Draft, Methodology. K. León-López: Conceptualization, Resources, Writing - Review & Editing, Data Curation. P. Goyes-Peñañiel: Writing - Review & Editing, Investigation, Conceptualization, Resources. L. Galvis: Writing - Review & Editing, Supervision. H. Arguello: Writing - Review & Editing, Supervision, Project administration.

All authors have read and agreed to the published version of the manuscript.

## Data Availability

The datasets and codes are accessible at <https://github.com/luismiguel13/DIPsgr>

## Conflicts of Interest

The authors declare no conflict of interest.

## Institutional Review Board Statement

Not applicable.

## Informed Consent Statement

Not applicable.

## References

- [1] L. Hatton, M. H. Worthington, J. Makin, "Seismic data processing: theory and practice," Merlin Profiles Ltd., Tech. Rep., 1986.
- [2] N. Cooper, L. A. Briceño, L. Alfredo, M. Vides, *Manual para la adquisición y procesamiento de sísmica terrestre y su aplicación en Colombia*. Colombia: Universidad Nacional de Colombia, 2010. [Online]. Available: [https://www.anh.gov.co/documents/34/Manual\\_Tecnica\\_s\\_Sismica\\_Terrestre.pdf](https://www.anh.gov.co/documents/34/Manual_Tecnica_s_Sismica_Terrestre.pdf)
- [3] C. L. Liner, *Elements of 3D seismology*. Society of Exploration Geophysicists, 2016.
- [4] X. Wang, S. Yu, "Seismic Data Regularization on Nonequispaced Grid via a Joint Sparsity-Promotion Method," *IEEE Geoscience and Remote Sensing Letters*, vol. 19, pp. 1–5, 2022, doi: <https://doi.org/10.1109/LGRS.2021.3072356>
- [5] W. Liu, S. Cao, G. Li, Y. He, "Reconstruction of seismic data with missing traces based on local random sampling and curvelet transform," *J. Appl. Geophys.*, vol. 115, pp. 129–139, 2015, doi: <https://doi.org/10.1016/j.jappgeo.2015.02.009>
- [6] P. Yang, J. Gao, W. Chen, "Curvelet-based POCS interpolation of nonuniformly sampled seismic records," *J. Appl. Geophys.*, vol. 79, pp. 90–99, 2012, doi: <https://doi.org/10.1016/j.jappgeo.2011.12.004>

- [7] F. Kong, F. Picetti, V. Lipari, P. Bestagini, X. Tang, S. Tubaro, “Deep Prior-Based Unsupervised Reconstruction of Irregularly Sampled Seismic Data,” *IEEE Geosci. Remote Sens. Lett.*, vol. 19, pp. 1–5, 2022, doi: <https://doi.org/10.1109/LGRS.2020.3044455>
- [8] Q. Liu, L. Fu, M. Zhang, “Deep-seismic-prior-based reconstruction of seismic data using convolutional neural networks,” *Geophysics*, vol. 86, no. 2, pp. V131–V142, Mar. 2021, doi: <https://doi.org/10.1190/geo2019-0570.1>
- [9] N. Kazemi, E. Bongajum, M. D. Sacchi, “Surface-Consistent Sparse Multichannel Blind Deconvolution of Seismic Signals,” *IEEE Trans. Geosci. Remote Sens.*, vol. 54, no. 6, pp. 3200–3207, 2016, doi: <https://doi.org/10.1109/TGRS.2015.2513417>
- [10] O. Villarreal, K. León-López, D. Espinosa, W. Agudelo, H. Arguello, “Seismic source reconstruction in an orthogonal geometry based on local and non-local information in the time slice domain,” *J. Appl. Geophys.*, vol. 170, p. 103846, 2019, doi: <https://doi.org/10.1016/j.jappgeo.2019.103846>
- [11] K. L. Lopez, J. M. Ramirez, W. Agudelo, H. Arguello Fuentes, “Regular Multi-Shot Subsampling and Reconstruction on 3D Orthogonal Symmetric Seismic Grids via Compressive Sensing,” in *2019 XXII Symposium on Image, Signal Processing and Artificial Vision (STSIVA)*, 2019, pp. 1–5. doi: <https://doi.org/10.1109/STSIVA.2019.8730279>
- [12] X. Chai, G. Tang, S. Wang, K. Lin, and R. Peng, “Deep Learning for Irregularly and Regularly Missing 3-D Data Reconstruction,” *IEEE Trans. Geosci. Remote Sens.*, vol. 59, no. 7, pp. 6244–6265, 2021, doi: <https://doi.org/10.1109/TGRS.2020.3016343>
- [13] S. Mandelli, F. Borra, V. Lipari, P. Bestagini, A. Sarti, S. Tubaro, “Seismic data interpolation through convolutional autoencoder,” in *SEG Technical Program Expanded Abstracts 2018*, Aug. 2018, no. October, pp. 4101–4105. doi: <https://doi.org/10.1190/segam2018-2995428.1>
- [14] S. Mandelli, V. Lipari, P. Bestagini, S. Tubaro, “Interpolation and Denoising of Seismic Data using Convolutional Neural Networks,” arXiv.org, pp. 1–17, Jan. 2019, doi: <https://doi.org/10.48550/arXiv.1901.07927>
- [15] D. Kuijpers, I. Vasconcelos, and P. Putzky, “Reconstructing missing seismic data using Deep Learning,” arXiv.org, Jan. 2021, doi: <https://doi.org/10.48550/arXiv.2101.09554>
- [16] J. D. Kelleher, “Deep learning,” *Mit Press Essential Knowledge Series*, vol. 1, 2019.
- [17] D. Ulyanov, A. Vedaldi, V. Lempitsky, “Deep Image Prior,” *Proceedings of the IEEE conference on computer vision and pattern recognition*, 2018, pp. 9446–9454, doi: <https://doi.org/10.1109/CVPR.2018.00984>
- [18] B. Wang, W. Lu, “Accurate and efficient seismic data interpolation in the principal frequency wavenumber domain,” *J. Geophys. Eng.*, vol. 14, no. 6, pp. 1475–1483, 2017, doi: <https://doi.org/10.1088/1742-2140/aa82dc>
- [19] W. Xiongwen, W. Huazhong, Z. Xiaopeng, “High dimensional seismic data interpolation with weighted matching pursuit based on compressed sensing,” *J. Geophys. Eng.*, vol. 11, no. 6, p. 065003, 2014, doi: <https://doi.org/10.1088/1742-2132/11/6/065003>
- [20] Q. Wang, Y. Shen, L. Fu, H. Li, “Seismic data interpolation using deep internal learning,” *Exploration Geophysics*, vol. 51, no. 6, pp. 683–697, 2020, doi: <https://doi.org/10.1080/08123985.2020.1748496>
- [21] P. Goyes-Peñañiel, E. Vargas, C. V. Correa, W. Agudelo, B. Wohlberg, H. Arguello, “A Consensus Equilibrium Approach for 3-D Land Seismic Shots Recovery,” *IEEE Geosci. Remote Sens. Lett.*, vol. 19, pp. 1–5, 2022, doi: <https://doi.org/10.1109/LGRS.2021.3082421>
- [22] F. Luperini et al., “Architecture and Performance of Devito, a System for Automated Stencil Computation,” *ACM Trans. Math. Softw.*, vol. 46, no. 1, pp. 1–28, 2020, doi: <https://doi.org/10.1145/3374916>
- [23] R. Versteeg, “The Marmousi experience: Velocity model determination on a synthetic complex data set,” *Lead. Edge*, vol. 13, no. 9, pp. 927–936, 1994, doi: <https://doi.org/10.1190/1.1437051>
- [24] Robert G. Keys and Douglas J. Foster, “Mobil AVO viking graben line 12,” 2023. [Online]. Available: [https://wiki.seg.org/wiki/Mobil\\_AVO\\_viking\\_graben\\_line\\_12](https://wiki.seg.org/wiki/Mobil_AVO_viking_graben_line_12)

[25] G. B. Madiba, G. A. McMechan, “Processing, inversion, and interpretation of a 2D seismic data set from the North Viking Graben, North Sea,” *Geophysics*, vol. 68, no. 3, pp. 837–848, May 2003, doi: <https://doi.org/10.1190/1.1581036>

[26] P. Goyes-Peñafiel et al., “Coordinate-Based Seismic Interpolation in Irregular Land Survey: A Deep Internal Learning Approach,” *IEEE Trans. Geosci. Remote Sens.*, vol. 61, pp. 1–12, 2023, doi: <https://doi.org/10.1109/TGRS.2023.3290468>

[27] D. P. Kingma, J. Ba, “Adam: A Method for stochastic optimization,” arXiv preprint arXiv:1412.6980, pp. arXiv–1412, 2017. [Online]. Available: <https://arxiv.org/abs/1412.6980>